Case Study

Flood Routing Simulation and System Customization for a High-Leakage River Channel in China

Shuai Song[1]; Xilai Zheng[2]; Fadong Li, Ph.D.[3]; Shoubo Tian[4]; and Guoqing Lin[5]

Abstract: Leakage is a major factor impacting the evolution of flood in a highly permeable river. By integrating a mathematical model with data provided by a monitoring database, a flood routing system was developed for the Dagu River in China. The aim of this study was to calculate the leakage discharge and to discuss the effect of leakage for flood modeling within a high-leakage riverbed. This system was implemented for application of a flood-diversion experiment in 2003, which accessed data automatically and used estimated coefficients to calculate leakage discharge. The results showed that simulated discharge values fit well with the measured values, with an average relative error less than 10%, and the leakage average relative error was approximately 2%. The infiltration experiments showed that the leakage coefficient could be treated as a constant when the dynamics in the initial phase of a short flood event was stimulated. The initial water level and leakage and roughness coefficients were the main factors required to accurately determine the discharge of river seepage.
DOI: 10.1061/(ASCE)HY.1943-7900.0000710.

CE Database subject headings: Flood routing; River beds; Leakage; Coefficients; Roughness; Coefficients; China; Simulation.

Author keywords: Flood routing; Riverbed leakage; Leakage coefficient; Roughness coefficient.

Introduction

Water is increasingly becoming a scarce resource in many parts of the world, and one important aspect for improving management of water resources is increased understanding of the processes involved in flash-flood warnings (Montz and Gruntfest 2002). Several structural (i.e., dams, dikes, levees, and embankments) and nonstructural (i.e., flood plain regulations and flood warning systems) methods have been proposed to manage flood risk and to reduce the adverse consequences of floods. Furthermore, the introduction of flood routing systems has become an indispensable part of the flood risk management (Aly and Eric 2007). Flood routing can support response strategies and provide reliable predictions for decisions to mitigate flood-related damage, frequency of flood events, their consequences, etc.

[1]Key Laboratory of Ecosystem Network Observation and Modeling, Institute of Geographic Sciences and Natural Resources Research, Chinese Academy of Sciences, Beijing 100101, China; and Graduate Univ. of Chinese Academy of Science, Beijing 100049, China. E-mail: frysoo@163.com

[2]Key Laboratory of Marine Environmental Science and Ecology, Ministry of Education, Ocean Univ. of China, Qingdao 266003, China. E-mail: zhxilai@ouc.edu.cn

[3]Professor, Key Laboratory of Ecosystem Network Observation and Modeling, Institute of Geographic Sciences and Natural Resources Research, Chinese Academy of Sciences, Beijing 100101, China (corresponding author). E-mail: lifadong@igsnrr.ac.cn

[4]Key Laboratory of Marine Environmental Science and Ecology, Ministry of Education, Ocean Univ. of China, Qingdao 266003, China. E-mail: tianshoubo@ouc.edu.cn

[5]Key Laboratory of Marine Environmental Science and Ecology, Ministry of Education, Ocean Univ. of China, Qingdao 266003, China. E-mail: steedlgq@163.com

Note. This manuscript was submitted on July 25, 2011; approved on November 16, 2012; published online on November 20, 2012. Discussion period open until November 1, 2013; separate discussions must be submitted for individual papers. This paper is part of the ***Journal of Hydraulic Engineering***, Vol. 139, No. 6, June 1, 2013. © ASCE, ISSN 0733-9429/2013/6-656-663/$25.00.

The hydrological and hydraulic methods are bases for the assessment, utilization, and protection of water resources. The comprehension of these bases is the core of flood routing research. At present, two methods are commonly used to predict flood events, namely, (1) analysis of a selected set of hydro-meteorological parameters, e.g., the artificial neural networks (Ahmad and Simonovic 2006; Panda et al. 2010); and (2) implementation of mathematical models (Pedregal 2009; Liu et al. 2008; Romanowicz et al. 2008). These methods have been used to improve water flow routing, flood forecast, and flood risk management. Ahmad and Simonovic (2006) developed an intelligent decision support system for different phases of flood management, from rapid updates of flood forecasts to flood impact estimation. Large-scale integrated hydrologic modeling systems have also been established. For example, the object modeling system (Kralisch et al. 2005) provided a modeling framework for management of water resources based on several models in a joint approach. In the same way, some of the most frequently used models are *MIKE* (Denmark), *HEC-RAS* (United States), *SOBEK* (Netherlands), *DRAINS* (Australia), and *Aquaveo SMS* (United States).

The interaction between groundwater and river plays an important role in modeling the hydrological cycle in a river basin. In particular, the infiltration flux from river to groundwater should not be omitted at a sandy gravel riverbed even in the absence of a clogging layer (Anderson 2005). However, the estimation of leakage coefficient is difficult in both surface water and groundwater modeling (Doppler et al. 2007). The infiltration rate of river water can be measured by seepage meters and assessed by discharge measurements along a river. Kaleris (1998) discussed these two methods for estimating the leakage rate from small streams to groundwater. Zechner and Frielingsdorf (2004) applied hydraulic head and seepage flux data to calibrate the model in a riverbed with strong river–aquifer interaction. Using the SPRING model in a high-leakage area, Doppler et al. (2007) found that major flood events had a persistent influence on the river–aquifer interaction, and leakage coefficients should be treated as a time-dependent variable. The previous studies primarily focused on methods of flood

J. Hydraul. Eng. 2013.139:656-663.

processes, leakage coefficients in clogging processes, interactions between groundwater and surface water, and flood loss. However, few studies have addressed flood routing in high-leakage riverbeds and the effect of high-leakage rate in this flood process.

This study addresses the parameters related to accurate calculation of leakage discharge to improve flood routing simulations, and provides strategies to increase data access and user convenience. The purposes of this paper are (1) to model flood routing considering high-leakage rate and customize a program that is able to realize data access automatically and achieve statistical analysis of floods; (2) to discuss the effect of various parameters on leakage discharge; and (3) to understand the effect of leakage coefficient on modeling floods in high-leakage riverbed in typically monsoon-controlled regions.

Site Description

The Dagu, the longest river in the Shandong peninsula, is approximately 179.9 km long. Its basin covers 4,850.7 km^2 in Qingdao, southwards into Jiaozhou Bay. After entering the northern boundary of Qingdao, the river receives more water from reservoirs such as the Chanzhi reservoir in the upper reach, which is the largest one, and main tributaries such as the Zhu, Xiaogu, Wugu, Luoyao, and Liuhao Rivers (Fig. 1). The upper reach of the river basin, with a flat topography and elevation of 20–50 m, is mainly composed of clastic and volcanic rock. The middle and lower reaches along the river valley are alluvial plains, with an elevation in the range of 4–40 m. The river valley is flat terrain with a gradient of 0.7–2‰ and a slight southwards tilt. The average width of the downstream valley is 6 km and riverbed depth is approximately 2 m.

Mean annual precipitation from 1956 to 2003 in this basin was 675.6 mm, with 73% of precipitation falling from July to September. The Dagu River has two remarkable characteristics, namely, (1) the relatively concentrated precipitation period raises water level significantly, with zero flow after a short flood event and dry conditions during the dry season, and (2) a very high leakage rate. Since the 1960s, there were two flood events that had peak discharges exceeding 3,000 m^3/s, and eight events exhibited discharges over 2,000 m^3/s. According to a water-diversion experiment conducted in 2003, the total discharge was 54.33×10^6 m^3, with a leakage of 68.6%, due to a wide, shallow, and sandy bed in the Dagu River.

Fig. 1. Location of the Dagu River and leakage coefficient zones (1–3) for the model

System Design

Model

The *MIKE 11* hydrodynamic (HD) module is a one-dimensional modeling tool that has been widely used in flood routing studies throughout the world (Henrik and Clus 2005; Monninkhoff and Zhijia 2009; Rabuffetti and Barbero 2005; Turan and Burak 2006). It can be applied for hydraulic analysis of a flood, using an implicit finite difference scheme for the computation of unsteady flows in rivers and estuaries. Furthermore, it provides interfaces to build user applications with MIKEOBJECTS, which is a component object model (COM) object accessing the components from most programming languages.

System Components

Fig. 2 illustrates the architecture of the flood system components. The popular three-tier client–server architecture was deployed. Microsoft *.NET Framework 2.0* and *C# server* were used as the platform and programming language, respectively. In addition, it requires COM groupware, which can be run on the. *NET* platform. On the server site, *MSSQL Server 2000* serves as the workstation to facilitate data storage and retrieval on the *Windows Server 2003* operating system (Liberty 2005).

Functionality

Considering the characteristics of the Dagu River flood routing, the functions of this system contain basic conditions, hydrologic modeling, and data analysis. This system provides lots of flood routing parameters for users. These parameters include initial conditions, boundary conditions, roughness coefficient, leakage coefficient, initial water level, start and end simulation times, selection of units, and so on. Time series (TS) data can be obtained

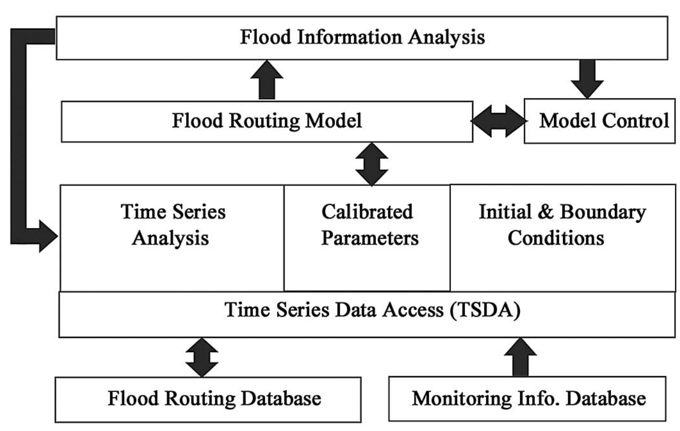

Fig. 2. Schematic layout of the flood system framework

J. Hydraul. Eng. 2013.139:656-663.

from users' manual inputs or automatically from the monitoring database. Within the HD module framework, *C#* was used to customize applications and create properly constructed batch files that contain native disk operating system commands and allows running multiple models sequentially. Data analysis includes the visual operation of river catchment, statistic analysis of results, abnormal mutations analysis, and alarm while exceeding the warning level.

Data Access and Model Control

One of the most important data types in HD is the TS, which is used as both input and output. Most of input/output data are provided in regular TS formats. To meet the needs of complex database formats (Alfredsen and Sæther 2000), time series data access (TSDA) was a hierarchy of input/output class libraries, which is based on the Time Series Package that is one part of MIKEOBJECT. However, in order to realize automatic data access, some special classes were designed based on MIKEOBJECT. For example, *globalTSObject* keeps the basic TS information and contains a reference to *globalTSConnection* that is responsible for connecting with basic TS files and databases. The *MFiltrate* class is responsible for the non-equidistant TS data obtained from monitoring databases by filtering data automatically to confirm the soundness of the simulation process.

The flood routing simulation is based primarily on a HD module that solves the nonlinear equations of open-channel flow (Saint-Venant equation) using an implicit finite difference scheme (DHI MIKE 2007; Rodríguez et al. 2006). Eqs. (1)–(3) are the parts of *MIKE 11*. Eq. (4) was designed independently in the system to check the water balance results and to calculate leakage discharge in a certain range of channel automatically.

$$\frac{\partial A}{\partial t}+\frac{\partial Q_s}{\partial L}+\frac{\partial Q_r}{\partial L}=q \tag{1}$$

$$\frac{\partial Q_s}{\partial t}+\frac{\partial(a\frac{Q_s^2}{A})}{\partial L}+gA\frac{\partial h}{\partial L}+g\frac{Q_s|Q_s|}{C^2AR}=0 \tag{2}$$

$$Q_r=l_c\times\Delta h \tag{3}$$

$$Q_r=Q_u+Q_a-Q_1-Q_c \tag{4}$$

where A = flow area; t = time; Q_s = horizontal discharge; Q_r = leakage discharge; q = lateral inflow; h = stage above datum; C = Chézy resistance coefficient; R = hydraulic radius; L = distance; g = acceleration of gravity; l_c = leakage coefficient; Δh = head difference between the river and the aquifer below the river; a = momentum distribution coefficient; Q_u = inflows in the upper section; Q_l = outflows in the lower section; Q_a = branch inflows; and Q_c = discharge variety referring to the initial and end water volume in the channel.

Data and Parameters

Approximately 2,000 detailed geographic information system (GIS) data in 180 cross sections were directly converted into a specific GIS format that can be recognized by the HD model. The export discharge of the Chanzhi reservoir (initial condition) and water levels and discharge (boundary conditions) of six tributaries could be obtained from a monitoring system and converted into DFS0 format files using TSDA. The monitoring system was managed by the Qingdao Municipal Bureau of Hydrology. It stores data in all catchments, such as reservoir operation information, water level.

Leakage coefficients were estimated from field and laboratory experiments, and then roughness coefficients and leakage coefficients were calibrated using observed water level and discharge from the parameters in the sand mining report (Li 2005). The leakage discharge can be used as verification results to assess the correctness of the leakage coefficients.

Roughness coefficient was used to calibrate the calculation model by matching the observed routing curve with the one obtained from the model (Turan and Burak 2006). Most sections of the Dagu River are usually dry and covered with weeds before the flood season, and therefore, river water is quick to seep after a flood event. According to the sand mining report, the roughness coefficient varied from 0.03 to 0.042 (Li 2005). Considering the river hydraulic characteristics, cross-sectional geometry shape, and riverbed characteristics in different sections from the sand mining report (Li 2005; Romanowicz et al. 2008), two values of roughness coefficient were selected and subject to calibration using the measured data; these were 0.038 in the upstream of Yifeng, and 0.041 in the downstream region. A trial-and-error process was used for parameter adjustment to come up with a match between simulated and observed values. According to the calibration results, the calibrated roughness coefficients were a little larger than the mean values suggested by the reports. The dry riverbed and lots of weeds in the riverbed were the main possible reasons that led to the large calibrated roughness coefficient.

Estimation of leakage discharge is impacted by the selected leakage coefficient (Doppler et al. 2007). It is hard to estimate the leakage discharge at a small scale for an entire river without setting precise leakage coefficients for each section. To study the leakage regularity, three representative sites were chosen based on the criterion of riverbed soil characteristics for pilot leakage tests over 3–4 h. A rectangular tank measuring $4\times0.8\times0.3$ m was dug into the riverbed. The rectangular tank had a 90° V notch on its two short vertical sides and was covered with a thin plastic film. Pumps were used to inject water into the tank. When the water was stable, the plastic film was quickly removed. Leakage rate could be calculated according to the results of the pilot experiment (Fig. 3). Considering the pilot leakage experiments results, including the factors of river width and gradient, the channel was divided into three zones (Fig. 1), with estimated leakage coefficients of 4.8×10^{-7}, 4.1×10^{-7}, and 3.8×10^{-7} s^{-1}, respectively. Similarly, estimated data of leakage coefficients were also reported with higher seepage (Doppler et al. 2007).

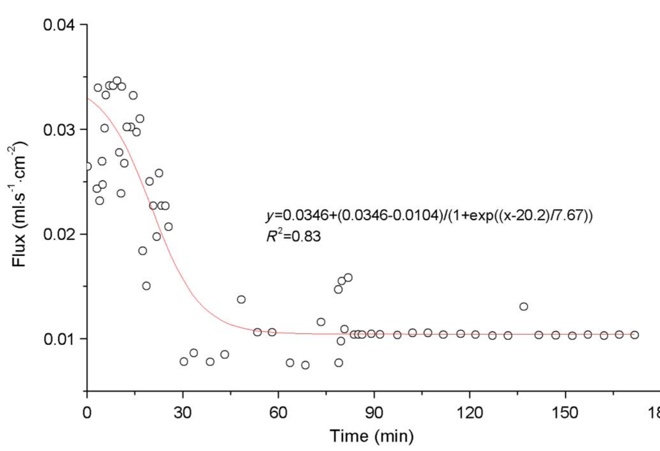

Fig. 3. Leakage flux variability for an initial dry bed at the Yubi site

Results and Discussion

Experiments Results

The pilot experiments provided data that allowed to determine how much impact the unsaturated leakage had on the total leakage discharge of the flood event. For example, at the Yubi site, the initial infiltration capacity was large but the capacity stabilized just about 1 h later. Results showed that the maximum leakage flux was 30.2 m^3/dm^2 and the stable leakage flux was approximately 8.6 m^3/dm^2 at the Yubi site. The unsaturated filtration time (Fig. 3) was much shorter than flood duration, and the leakage discharge on the unsaturated condition accounted for 1.0% of the whole leakage discharge. Therefore, the stable infiltrative flux was used to calculate the leakage capacity and the leakage coefficients were simplified as constant values in the model.

Five observation wells were arranged beside the river, at Shawanai, Guozhuang, Nancun, Nancunshuili, and Daguhesuo (Yu et al. 2003). Groundwater table was measured four times on April 21, April 26, May 1, and May 6 in 2003. The maximum increase of groundwater table was 1.41 m at the Daguhesuo site in the downstream, and the groundwater table of the other sites rose from 0.17 to 0.24 m. In addition, the groundwater table of 18 sites away from the river channel changed from 0 to −0.22 m. Groundwater tables were 2.5–3.1 m at the upstream and 0.6–2.5 m at the downstream sections. Yu et al. (2003) reported the details of the groundwater tables. Groundwater tables were not monitored during infiltration experiment, and therefore the values measured on April 21, 2003 were used, because the groundwater table changed very little before the rainy season.

Experiments generated a range for leakage coefficient for the Dagu River. Because it is difficult to perform replicate analyses of floods to confirm these values, the range determined by the distinctly variable upstream and downstream regions of the river was used for modeling purposes. The leakage coefficients obtained from pilot experiments were compared with hydraulic conductivities estimated from the soil samples using the Hazen formula [Eq. (5)] (Blaschke et al. 2003):

$$K = 0.0116 d_{10}^2 (0.7 + 0.03T) \tag{5}$$

where K = hydraulic conductivity (m/s); d_{10} = representative grain diameter (10% of the sediment mass are smaller than d_{10}); and T = water temperature.

The grain compositions above 20-cm mixed sands were measured at Shanghaiba, Yujiaxiaoli, Yubi, Yifeng, and Nanshaliang and some 0–10-cm mixed sands were also measured. The grain compositions of the clogging layer (<1 cm) were measured only in Yujiaxiaoli, Yubi, and Nanshaliang. The grain compositions were used to estimate the hydraulic conductivities [Eq. (5)]. Leakage coefficient l_c (s^{-1}) is often combined to a K as follows: $l_c = K/d$, where K and d are hydraulic conductivity and thickness of the riverbed, respectively (Doppler et al. 2007). For example, the bulk density above 20-cm mixed sand at Yubi was approximately 1.37 g/cm^3. Saturated condition was assumed in this flood case. Approximately 3 m was used as the thickness of riverbed in Yubi site. The d_{10} of 0–10-cm mixed sand at Yubi was 0.085 mm and the hydraulic conductivity was 8.4×10^{-5} m/s according to Eq. (5), while the leakage coefficient at the Yubi site was 2.6×10^{-5} s^{-1}. These values were similar to the results of the infiltration experiments. However, the hydraulic conductivity of the clogging layer (<1 cm) was 1.2×10^{-6} m/s and the leakage coefficient was 3.9×10^{-7} s^{-1} [Eq. (5)]. The reason for obtaining different leakage coefficients is that the hydraulic conductivity of the clogging layer is smaller than the hydraulic conductivity of the aquifer because of clogging processes, i.e., the clogging layer controls the leakage rate (Doppler et al. 2007). Leakage coefficients of 0–20-cm mixed sand in Shanghaiba, Yujiaxiaoli, Yubi, Yifeng, and Nanshaliang were 4.8×10^{-5}, 9.6×10^{-5}, 2.9×10^{-5}, 3.5×10^{-5}, and 7.3×10^{-5} s^{-1}, respectively. Leakage coefficients of the clogging layer (<1 cm) in Yujiaxiaoli, Yubi, and Nanshaliang were 8.7×10^{-7}, 3.9×10^{-7}, and 4.2×10^{-7} s^{-1}, respectively. Trends of hydraulic conductivity in the vertical direction were similar to the results reported by Blaschke et al. (2003) in a high-leakage area. Leakage coefficients at 0–1-cm and 0–20-cm mixed sand were approximately 10^{-7} to 10^{-8} s^{-1} and 10^{-5} to 10^{-6} s^{-1}, respectively, which was in accordance with the estimated results. This estimated method is affected by the thickness of riverbed and the clogging layer, and therefore it can be used only when these values have been measured.

Flood Routing and Leakage

When the sluice gates of the reservoir were open, discharge data of monitoring sections were manually monitored by the current meter method. All the data were stored in the database. Statistical information of the measured daily mean discharge in the representative sites is shown in Table 1. The measured data of the flood hydrograph exhibited typical features (Fig. 4). It is relatively flat due to large reservoir water regulation. The riverbed was dry before the flood event. The time of rising limb was very short, approximately 8 h in the Jiangjiazhuang and Nancun sections. The time of falling limb was short at the upstream sections, whereas it was relatively long at the downstream sections. After the flood, the base flow of the river was again zero.

Statistics of inflow, outflow, and water storage in every monitoring section are shown in Table 2. A water balance analysis was performed using this information. The sluice gates and upstream dam held back a total of 8,380,000 m^3. Water loss, including seepage and evaporation, was 37,280,000 m^3 in route, and the inflow at the Jihongtan reservoir was 11,170,000 m^3. Leakage discharge was 37.11×10^6 m^3, 68.6% of the total flow.

The data during the period from April 22, 2003 to May 10, 2003 were used to check the model data sets and the precision of flood routing. If the sediment is unsaturated, the channel leakage is initially large and then gradually shifts to a relatively stable value. However, seepage stabilizes after approximately 1 h and the riverbed soil becomes saturated, driven by a rubber dam collapse before

Table 1. Descriptive Statistics of Measured Daily Mean Discharge in the Representative Sites

Sites	Measured date (flow $\neq$ 0)	Maximum daily mean discharge (m^3/s)	Minimum daily mean discharge (m^3/s)	Average daily mean discharge (m^3/s)
Gejiabu	4/22–5/4	21.9	2.31	13.3
Chengjiaxiaoli	4/23–5/4	44.0	3.36	25.4
Shawanzhuang	4/23–5/4	58.4	8.68	35.8
Nancun	4/25–5/4	44.8	18.5	38.3
Yinhuangzha	4/25–5/8	30.4	0.70	16.6

J. Hydraul. Eng. 2013.139:656-663.

Table 2. Statistics of Inflow, Outflow, and Water Storage in the Monitoring Sections

Segments	Inflow (10^4 m^3)	Sluice sites	Water storage (10^4 m^3) After flood	Before flood	Changes	Loss (10^4 m^3)	Outflow (10^4 m^3)
Beiye reservoir–Gejiabu	2,333	Longhushan	0	40	−40	763	1,610
Chanzhi reservoir–Chengjiaxiaolv	3,100	Jiangjiazhuang	30	30	0	252	2,848
Gejiabu–Houshawanzhuang	4,458	Houshawanzhuang	10	0	10	429	4,019
Houshawanzhuang–Nancun	4,019	Yuanjiazhuang	20	0	20	699	3,310
		Yifeng	30	0	30		
		Yatou	80	120	−40		
Nancun–Yinhuangzha	3,310	Chahe	200	60	140	1,197	1,865
		Yinhuang	108	0	108		
Yinhuangzha–Jinghongtan reservoir	1,865	Jiatuan	360	0	360	388	—
		Jihongtan reservoir	1,117	0	1,117		
		Total	1,955	250	1,705	3,728	—

the flood event. The effect of initial soil retaining capacity was neglected in the flood event modeling. The computing time step was set to 1 min and the boundary and initial conditions were selected from the database. The export discharge of the Chanzhi reservoir was regarded as the initial condition. Water levels and the discharge of tributaries were treated as boundary conditions.

The initial steady-state conditions were recommended for each simulation before the unsteady testing (Clemmens et al. 2005). The model assumed that they can approach initial steady-state conditions with a zero discharge boundary condition through the unsteady flow model for the study of water level and discharge at the gate positions. A period of initial steady flow at the start of this simulation was established and results showed that the water levels and discharges did not appear to drift at every section. Water levels at Jiangjiazhuang and discharges at Jiangjiazhuang and Nancun (Fig. 5) presented examples of three scenarios with different initial steady conditions.

Two sections, Shawanzhuang and Nancun, were selected to compare the water level and discharge results. Water levels and discharges were measured 27 times at Jiangjiazhuang, and 28 times at Nancun. Simulated accuracy was evaluated by the relative error, which is the quotient between the absolute error and the reference value. The average relative error of water level was less than 5% and the relative error of discharge was approximately 9%. The relative error of rising-side time and the time to peak was less than 0.5%. Fig. 4 indicates the model performances in predicting the water level; peak flow and time of peak were predicted very well. However, the predicted water level was larger than the measured value at the Nancun section, but approximately 0.15 m lower at the Shawanzhuang section. These two sections had different roughness coefficients (0.038 and 0.041 at Shawanzhuang and Nancun, respectively), which may explain the different behaviors of these sections. Another possible reason is the error between observed riverbed elevation and GIS data provided by the river sand mining report. Similar water-stage error was also reported in other simulations (Panda et al. 2010).

The river channel was divided into five zones to analyze the leakage discharge. Table 3 shows the simulated and measured leakage value in each river segment. The average relative error was approximately 2%. The upstream leakage discharge was smaller than that of the downstream, because the watercourse was narrow and with higher velocity. By contrast, the leakage discharge was large between Nancun and Jiatuan due to a wide watercourse and an uneven and ruderal riverbed. These results suggest that hydrograph characteristics and leakage can be well estimated using the current input parameters, and that the model successfully reflects the real flood routing situation.

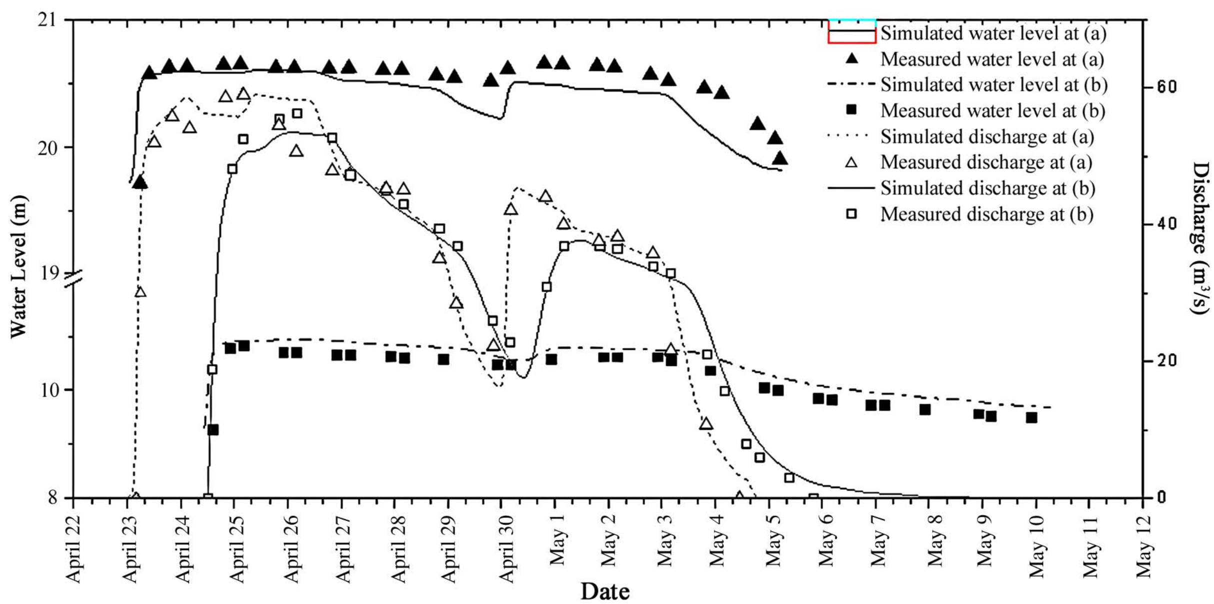

Fig. 4. Comparison of measured and simulated values in the (a) Shawanzhuang; (b) Nancun sections

J. Hydraul. Eng. 2013.139:656-663.

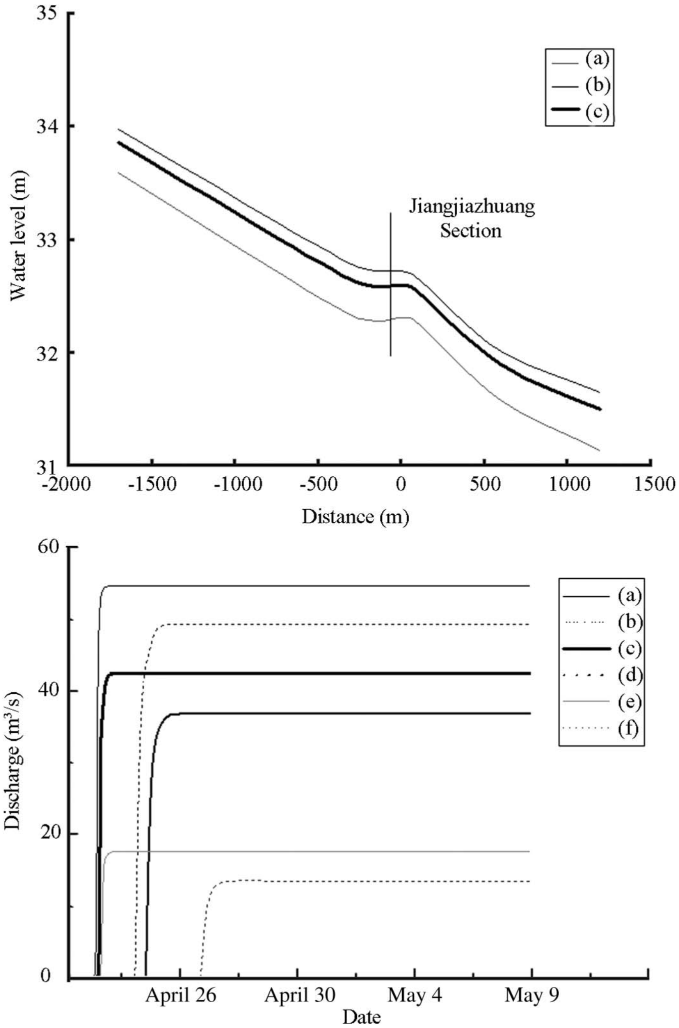

Fig. 5. Simulation results with different initial steady conditions for water levels at Jiangjiazhuang and discharges at Jiangjiazhuang and Nancun: (a) Jiangjiazhuang section, initial discharge $= 60\ m^3/s$; (b) Nancun section, initial discharge $= 60\ m^3/s$; (c) Jiangjiazhuang section, initial discharge $= 46.3\ m^3/s$; (d) Nancun section, initial discharge $= 46.3\ m^3/s$; (e) Jiangjiazhuang section, initial discharge $=$ $20\ m^3/s$; (f) Nancun section, initial discharge $= 20\ m^3/s$; all the simulations are shown with no boundary inflows and gate constraints

Table 3. Comparison of Measured and Simulated Leakage Discharge in the River Segments

River segments	Simulated value ($10^4\ m^3$)	Measured value ($10^4\ m^3$)
Chanzhi–Chengjiaxiaolv	255	252
Chengjiaxiaolv–Houshawanzhuang	89	93
Houshawanzhuang–Nancun	721	699
Nancun–Yinhuangzha	1,164	1,197
Yinhuangzha–Jiatuan	392	388

Sensitivity Analysis

The objective of sensitivity analysis is to monitor the changes in response to the flood routing model due to changes in the value of the specified parameters. Channel leakage discharge is influenced by watershed parameters, including the initial soil water–retaining capacity, initial water level, roughness and leakage coefficients. In this model, sensitivity analysis was conducted to test the effects of realistic ranges of parameters on leakage discharge and the beginning time of rising limb (BTRL). Each parameter was performed by varying its values to study the effect while keeping the other parameters constant. The values of roughness coefficient, initial water level, and leakage coefficient were held constant as 0.038, 0 m and $3.80 \times 10^{-7}\ s^{-1}$, respectively.

Four roughness coefficients, such as 0.020, 0.025, 0.030, and 0.038 were selected to evaluate the effect on leakage discharge and the BTRL. There was a positive relationship between the Manning's n and leakage discharge, as well as between Manning's n and BTRL. The leakage discharge was found to increase by 44.90% as the roughness coefficient increased from 0.020 to 0.038 (Table 4). The BTRL was delayed by increasing the roughness coefficient (Table 4). When the roughness coefficient varied from 0.020 to 0.040, the BTRL at Jiangjiazhuang was delayed by 8.3 h. The reason is that an increase in the roughness coefficient induces microdepression storage and results in delayed initiation of the runoff process. Higher roughness coefficient also delayed the time to peak and prolonged the period of recession flow. Because the total runoff did not vary significantly, the total leakage discharge associated with high roughness coefficient was large throughout the whole flood process.

Initial water levels were increased from 0.0 to 0.8 m, with intervals of 0.2 m (Table 4), and leakage discharge was reduced proportionally from 2.55×10^6 to $1.43 \times 10^6\ m^3$. The reason is that water head was large at beginning of the flood event in this high-leakage area. When surface water began to seep into groundwater, groundwater table would increase and lead to a decrease in the water head, resulting in decrease of the seepage.

Leakage coefficient has a remarkable effect on leakage discharge (Table 4). The leakage discharge was found to increase linearly by increasing the leakage coefficient. An increase of leakage coefficient by 25.0% resulted in approximately 22.4% leakage discharge between the Chanzhi and Jiangjiazhuang sections. The effect of leakage coefficient appeared to be insignificant compared with that of the roughness coefficient toward the BTRL. The BTRL was moderately delayed with increasing leakage coefficient (Table 4). When roughness coefficients varied from 0.020 to 0.045, the BTRL at Jiangjiazhuang was delayed by 9.9 h, compared with only 2.5 h derived from varying the leakage coefficient from 2.40×10^{-7} to $55.50 \times 10^{-7}\ s^{-1}$. The reason is that an increase in infiltration would decrease the amount of runoff. The reduction in runoff delayed the BTRL, but the effect of delayed time of roughness coefficient appeared to be more sensitive than that of leakage coefficient.

Fig. 6 depicts the relationship of three parameters on leakage discharge between the Chanzhi and Jiangjiazhuang sections. Values on the left side of the vertical dotted line depict how the interaction of parameters effectively decreased the leakage discharge. However, leakage coefficient on the right side of the vertical dotted line was the main parameter that affected the leakage discharge, because initial water level was zero on the dry riverbed and the roughness coefficient, considered the realistic range, is already large. Leakage coefficient could potentially be increased due to effects of flood scour and sand mining in realistic conditions. The roughness coefficient controls leakage discharge due to its effects on river velocity and sluggish status, and thus the leakage discharge increases with increasing roughness coefficient. The flood routing process is complex and many factors affect the leakage discharge. A high leakage coefficient in the riverbed is a decisive condition of high leakage discharge, while high leakage discharge is also affected by other factors. The three factors of initial water level, leakage, and roughness coefficients should be considered to accurately determine leakage discharge.

J. Hydraul. Eng. 2013.139:656-663.

Table 4. Effect of Changes of the Values of Model Inputs on the Predicted Value

Parameters	Parameter values	Output parameters	Simulated values (difference)
Leakage coefficients ($\times 10^{-7}$ s^{-1})	2.4	Leakage discharge (Chanzhi–Jiangjiazhuang, 10^4 m^3)	138 (−45.9%)
	3.6		197 (−22.2%)
	4.8		255 (0)
	6.0		312 (22.4%)
	7.2		368 (44.3%)
Initial water level (m)	0	Leakage discharge (Chanzhi–Jiangjiazhuang, 10^4 m^3)	255 (0)
	0.2		244 (−4.3%)
	0.4		222 (−12.9%)
	0.6		188 (−26.3%)
	0.8		143 (−43.9%)
Roughness coefficient	0.020	Leakage discharge (Chanzhi–Jiangjiazhuang/ Jiangjiazhuang–shawanzhuang, 10^4 m^3)	176 (−31.0%)
	0.025		193 (−24.3%)
	0.030		210 (−17.6%)
	0.038		255 (0)
Leakage coefficients ($\times 10^{-7}$ s^{-1})	2.4	BTRL at Jiangjiazhuang (h)	18.1 (−0.7%)
	3.7		18.2 (−0.2%)
	18.5		19.0 (4.2%)
	37		19.8 (8.6%)
	55.5		20.6 (13.0%)
Roughness coefficient	0.020	BTRL at Jiangjiazhuang (h)	14.7 (−33.2%)
	0.025		17.3 (−21.4%)
	0.030		19.3 (−12.3%)
	0.040		23 (4.5)
	0.045		25 (13.6)

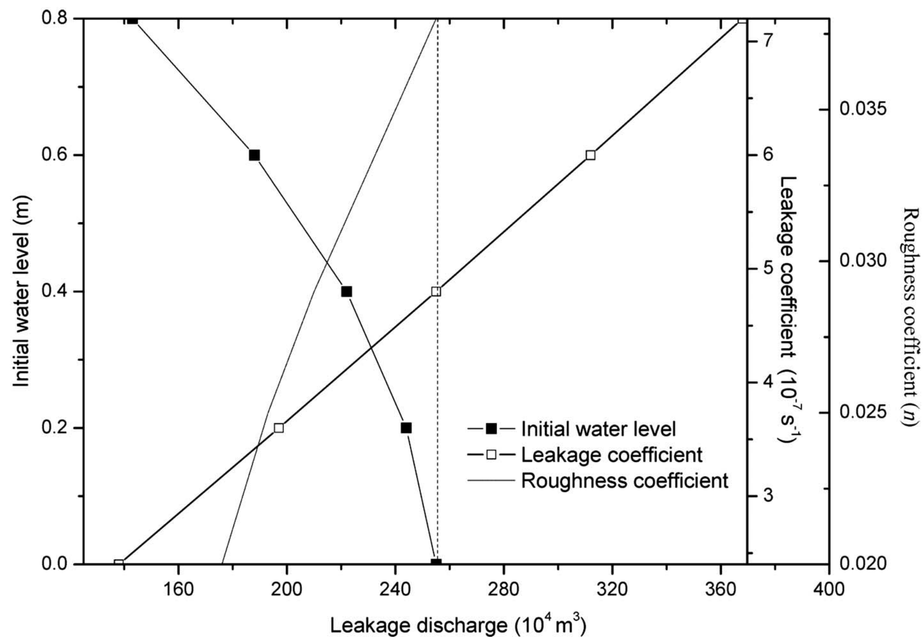

Fig. 6. Relationship of three parameters on leakage discharge between the Chanzhi and Jiangjiazhuang sections (the vertical dotted line denotes the parameters used in this case study)

Conclusions

To understand the effect of leakage coefficients for modeling flood routing in a high-leakage channel, a flood routing system considering leakage solution was developed for water resources management of the Dagu River. This system integrates MIKEOBJECT components and information provided by a monitoring database. Flood routing and leakage were well described by this model. The results of a leakage pilot field experiment were applied to the mathematical model to calculate leakage discharge in various river segments. The case study revealed the operational simplicity and high accuracy of the model. The average relative error of measured and simulated discharge was 10%, and average relative error of water level was less than 5%. The average relative error of simulated leakage discharge was only 2% for estimated parameters in each river segment. Leakage coefficient is a decisive

J. Hydraul. Eng. 2013.139:656-663.

condition of a high leakage discharge system, and leakage discharge increases significantly with increasing leakage coefficient. In addition, the initial water level and roughness coefficient are important for accurate calculations of seepage discharge.

In this case study, verification of the model is not mentioned due to lack of data. To reduce the risk of the model results, the most two important parameters, roughness and leakage coefficients, were carefully considered. The application of steady-state initial conditions was conducted for the robustness of the results. The reasonable range of leakage coefficients determined by the experiments was in accord with the calibrated results. Therefore, these experiments could provide the methods for proving the feasibility of leakage coefficient for a model in exiguous monitoring data area.

Acknowledgments

The project was financially supported by the 100 Talents Program of Chinese Academy of Sciences and the Municipal Bureau of Water Resources of Qingdao.

References

Ahmad, S., and Simonovic, S. P. (2006). "An intelligent decision support system for management of floods." *Water Resour. Manage.*, 20(3), 391–410.

Alfredsen, K., and Sæther, B. (2000). "An object-oriented application framework for building water resource information and planning tools applied to the design of a flood analysis system." *Environ. Model. Software*, 15(3), 215–224.

Aly, I. E.-K., and Eric, Y. (2007). "Modeling streamflows and flood delineation of the 2004 flood disaster, Mānoa, O'ahu, Hawai'i." *Pac. Sci.*, 61(2), 235–255.

Anderson, E. (2005). "Modeling groundwater-surface water interactions using the Dupuit approximation." *Adv. Water Resour.*, 28(4), 315–327.

Blaschke, A. P., Steiner, K.-H., Schmalfuss, R., Gutknecht, D., and Sengschmitt, D. (2003). "Clogging processes in hyporheic interstices of an impounded river, the Danube at Vienna, Austria." *Int. Rev. Hydrobiol.*, 88(3–4), 397–413.

Clemmens, A. J., Bautista, E., Wahlin, B. T., and Strand, R. J. (2005). "Simulation of automatic canal control systems." *J. Irrig. Drain. Eng.*, 131(4), 324–335.

DHI MIKE 11. (2007). "DHI MIKE 11 user and reference manual." Danish Hydraulic Institute, Hørsholm, Denmark.

Doppler, T., Franssen, H.-J. H., Kaiser, H.-P., Kuhlman, U., and Stauffer, F. (2007). "Field evidence of a dynamic leakage coefficient for modelling river–aquifer interactions." *J. Hydrol. (Amsterdam, Neth.)*, 347(1–2), 177–187.

Henrik, M., and Clus, S. (2005). "Adaptive state updating in real-time river flow forecasting—a combined filtering and error forecasting procedure." *J. Hydrol.*, 308(1–4), 302–312.

Kaleris, V. (1998). "Quantifying the exchange rate between groundwater and small streams." *J. Hydraul. Res.*, 36(6), 913–932.

Kralisch, S., Krause, P., and David, O. (2005). "Using the object modeling system for hydrological model development and application." *Adv. Geosci.*, 4, 75–81.

Li, S. (2005). *Sand mining planning in the Dagu River*, Water Conservancy Bureau of Qingdao, Qingdao, China (in Chinese).

Liberty, J. (2005). "Programming C#: Building .NET Applications with C#." O'Reilly Media, Incorporated.

Liu, C., Zheng, H., Zhang, L., and Wu, X. (2008). "Development of hydroinformatic modelling system and its application." *Sci. China Ser. E: Technol. Sci.*, 51(4), 456–466.

Monninkhoff, B. L., and Zhijia, L. (2009). "Coupling FEFLOW and MIKE11 to optimise the flooding system of the Lower Havel polders in Germany." *Int. J. Water*, 5(2), 163–180.

Montz, B. E., and Gruntfest, E. (2002). "Flash flood mitigation: Recommendations for research and applications." *Environ. Hazards*, 4(1), 15–22.

Panda, R. K., Pramanik, N., and Bala, B. (2010). "Simulation of river stage using artificial neural network and MIKE 11 hydrodynamic model." *Comput. Geosci.*, 36(6), 735–745.

Pedregal, D. J., Rivas, R., Feliu, V., Sa′nchez, L., and Linares, A. (2009). "A non-linear forecasting system for the Ebro River at Zaragoza, Spain." *Environ. Model. Software*, 24(4), 502–509.

Rabuffetti, D., and Barbero, S. (2005). "Operational hydro meteorological warning and real-time flood forecasting: The Piemonte Region case study." *Hydrol. Earth Syst. Sci.*, 9(4), 457–466.

Rodríguez, L. B., Cello, P. A., and Vionnet, C. A. (2006). "Modeling stream-aquifer interactions in a shallow aquifer, Choele Choel Island, Patagonia, Argentina." *Hydrogeol. J.*, 14(4), 591–602.

Romanowicz, R. J., Young, P. C., Beven, K. J., and Pappenberger, F. (2008). "A data based mechanistic approach to nonlinear flood routing and adaptive flood level forecasting." *Adv. Water Resour.*, 31(8), 1048–1056.

Turan, N. N., and Burak, U. A. E. (2006). "Flood forecasting and analysis within the Ulus Basin, Turkey, using geographic information systems." *Nat. Hazards*, 39(2), 213–229.

Yu, W. C., Fu, R. H., Chu, Y. B., and Sun, W. Y. (2003). *Monitoring report of water diversion in the Dagu River watershed*, Water Conservancy Bureau of Qingdao, Qingdao, China (in Chinese).

Zechner, E., and Frielingsdorf, W. (2004). "Evaluating the use of canal seepage and solute concentration observations for aquifer parameter estimation." *J. Hydrol.*, 289(1–4), 62–77.

J. Hydraul. Eng. 2013.139:656-663.